

Dynamical compactification of extra dimensions in the Euclidean type IIB matrix model: A numerical study using the complex Langevin method

Konstantinos N. Anagnostopoulos^a, Takehiro Azuma^b, Yuta Ito^c, Jun Nishimura^{cd} and Stratos Kovalkov Papadoudis^{*a}

^aPhysics Department, National Technical University,
Zografou Campus, GR-15780 Athens, Greece

^bInstitute for Fundamental Sciences, Setsunan University,
17-8 Ikeda Nakamachi, Neyagawa, Osaka, 572-8508, Japan

^cKEK Theory Center, High Energy Accelerator Research Organization,
1-1 Oho, Tsukuba, Ibaraki 305-0801, Japan

^dGraduate University for Advanced Studies (SOKENDAI),
1-1 Oho, Tsukuba, Ibaraki 305-0801, Japan

E-mails: konstant@mail.ntua.gr, azuma@mpg.setsunan.ac.jp,
yito@post.kek.jp, jnishi@post.kek.jp and sp10018@central.ntua.gr

The type IIB matrix model is conjectured to be a nonperturbative definition of type IIB superstring theory. In this model, spacetime is a dynamical quantity and compactification of extra dimensions can be realized via spontaneous symmetry breaking (SSB). In this work, we consider a simpler, related, six dimensional model in its Euclidean version and study it numerically. Our calculations provide evidence that the $SO(6)$ rotational symmetry of the model breaks down to $SO(3)$, which means that the theory lives in a vacuum where 3 out of the 6 dimensions are large compared to the other 3. Our results show the same SSB pattern predicted by the Gaussian expansion method and that they are in quantitative agreement. The Monte Carlo simulations are hindered by a severe complex action problem which is addressed by applying the complex Langevin method.

*Corfu Summer Institute 2018 "School and Workshops on Elementary Particle Physics and Gravity" (CORFU2018)
31 August - 28 September, 2018
Corfu, Greece*

*Speaker.

1. Introduction

Superstring theory is the most promising fundamental theory for the unification of all interactions, including gravity. The theory is defined in 10 spacetime dimensions and the connection to the real world, where 4 dimensions are macroscopic, is realized via compactification of the extra dimensions. This requires the introduction of many arbitrary parameters in the theory, leading to the problem of the string landscape. The IKKT or IIB matrix model [1], formally obtained by the dimensional reduction of ten-dimensional $\mathcal{N} = 1$ super-Yang-Mills theory to zero dimensions, is conjectured to be a non-perturbative definition of superstring theory in the large- N limit of the size of the matrices N . In this model, spacetime emerges dynamically from the eigenvalues of the bosonic degrees of freedom. Therefore, the scenario of the dynamical compactification of extra dimensions becomes possible. Monte Carlo simulations and analytic calculations using the Gaussian Expansion Method (GEM), provide evidence that dynamical compactification of extra dimensions occurs via Spontaneous Symmetry Breaking (SSB) of the rotational symmetry of space. Monte Carlo simulations [2–4] provide evidence that an infinite time emerges dynamically and 3 dimensional space undergoes expansion leaving the remaining 6 space dimensions small, showing that the model may realize phenomenologically interesting cosmology. The Euclidean version of the IIB model, obtained after a Wick rotation of the temporal dimension, has been studied using the GEM, providing evidence that dynamical compactification occurs via SSB of the $SO(10)$ rotational symmetry down to $SO(3)$ [5].

The Monte Carlo simulation of the Euclidean IIB matrix model, referred to simply as the IIB model in the following, can be thought of being the analog of lattice QCD simulations for superstring theory. Early attempts include the simulation of simpler, related models in lower dimensions or effective models that are thought to capture the central dynamical properties of the model that result in the SSB of the rotational symmetry [6–10]. The simulation of the IIB model is hindered by the complex action problem. The effective action which results after the integration of the fermionic degrees of freedom is complex, and it has been conjectured that the wild fluctuations of its complex phase is the reason that causes the SSB [11]. Configurations which are close to being lower dimensional result in milder fluctuations of the complex phase, therefore making them dominant in the path integral. This effect has been examined in [12–18]. It should be noted that the absence of the complex phase, like in the $D = 4$ IIB model [8, 10] or the phase quenched models [17, 18] implies absence of SSB. The complex action problem was addressed using a reweighting-based method [13], but it turned out to be very hard to determine the pattern of the SSB [18]. The complex Langevin method (CLM) [19, 20] has been applied successfully in several models with the complex action problem. CLM defines a stochastic process which can be used to calculate the expectation values of the observables. It is computationally simple, but it has the disadvantage of leading to wrong results in several known cases. Recent work [21–26] has clarified the conditions that are necessary and sufficient for justifying the CLM and has provided new techniques that make possible to meet these conditions for a larger space of parameters [27–34]. The CLM has been recently applied [31] to a simple matrix model with severe complex action problem [14] which has $SO(4)$ rotational symmetry that is expected to spontaneously break down to $SO(2)$ [35]. By deforming the original model, the singular drift problem [23] was avoided by the resulting shift of the eigenvalues of the Dirac operator away from zero [36]. By extrapolating back

to the original model, it was possible to reproduce the results of the GEM [35]. A similar problem occurs in many interesting problems with a complex fermionic effective action, like finite density QCD at low temperatures.

In this talk, we present the results in [37] where the work in [31] is extended to the 6D version of the IIB matrix model. This model suffers from a severe complex action problem due to a complex determinant appearing in the effective action after the integration of the fermionic degrees of freedom. GEM calculations provide evidence that the complex phase of the effective action causes SSB of the SO(6) symmetry down to SO(3) [38]. Using CLM and the methods employed in [31], we were able to reproduce the pattern of the SSB which was only marginally possible by using a reweighting-based method [17]. SSB is probed by perturbing the model with explicit SO(6) symmetry breaking operators $\langle \lambda_\mu \rangle$ representing the extent of spacetime in each direction, with the magnitude of the perturbation controlled by a parameter ε . ε is later extrapolated to 0 *after* taking the large- N limit. The singular drift problem is addressed by deforming the model with a fermionic operator with deformation parameter m_f . For finite m_f , the distribution of the eigenvalues is shifted away from 0 and the singular drift problem is avoided. This is checked directly by computing the eigenvalue distribution for small matrices, but it can also be easily checked for all of our measurements by applying a simple criterion proposed in [24]. In [24], it was shown that the singular drift problem does not appear when the distribution of the magnitude of the drift u is suppressed exponentially or faster for large values of u .

In order to obtain the SSB pattern, a careful extrapolation to the original model must be taken. First the large- N limit is obtained for finite m_f and ε values. Then, the limit $\varepsilon \rightarrow 0$ is taken in order to determine the SSB pattern for a given value of m_f . For finite m_f , SO(6) is explicitly broken down to SO(5). This is not a problem, however, because we are looking for SSB to SO(d) for $d < 5$. Finally the $m_f = 0$ extrapolation is taken and we find SSB to SO(3), with results that are quantitatively consistent with GEM.

These methods are currently applied to the original $D = 10$ dimensional IIB model [39]. In this case, GEM predicts that SO(10) is broken down to SO(3) instead of the desired SO(4) for a four dimensional spacetime [5] and a first principle calculation is desired. The success of the deformation method in the IIB model is encouraging attempts to apply it to other physically interesting systems with severe complex action problems, like in finite density QCD [40].

2. The Model

Our model is obtained by reducing the $\mathcal{N} = 1$ pure super SU(N) Yang-Mills theory in $D = 6$ dimensions to a point. One obtains a matrix model with $D = 6$ bosonic traceless Hermitian $N \times N$ matrices $(A_\mu)_{ij}$, $\mu = 1, \dots, 6$, $i, j = 1, \dots, N$ and $2^{D/2-1} = 4$ fermionic traceless $N \times N$ matrices with Grassmann entries $(\psi_\alpha)_{ij}$, $\alpha = 1, \dots, 4$. The action $S_b + S_f$ is given by the bosonic part S_b and the fermionic part S_f

$$S_b = -\frac{1}{4} N \text{tr} [A_\mu, A_\nu]^2 \quad (2.1)$$

$$S_f = N \text{tr} (\bar{\psi}_\alpha (\Gamma_\mu)_{\alpha\beta} [A_\mu, \psi_\beta]) , \quad (2.2)$$

and the model is defined by the partition function

$$Z = \int dA d\psi d\bar{\psi} e^{-(S_b + S_f)}. \quad (2.3)$$

The action is invariant under $SO(6)$ rotations, under which A_μ transform as a vector and ψ_α as a Weyl spinor. The 4×4 gamma matrices Γ_μ obtained after Weyl projection can be taken to be

$$\begin{aligned} \Gamma_1 &= i\sigma_1 \otimes \sigma_2, & \Gamma_2 &= i\sigma_2 \otimes \sigma_2, & \Gamma_3 &= i\sigma_3 \otimes \sigma_2, \\ \Gamma_4 &= i\mathbf{1} \otimes \sigma_1, & \Gamma_5 &= i\mathbf{1} \otimes \sigma_3, & \Gamma_6 &= \mathbf{1} \otimes \mathbf{1}, \end{aligned} \quad (2.4)$$

where σ_i , $i = 1, 2, 3$ are the Pauli matrices.

Integrating out the fermionic degrees of freedom, we obtain

$$\det \mathcal{M} = \int d\psi d\bar{\psi} e^{-S_f}, \quad (2.5)$$

where \mathcal{M} is a $4(N^2 - 1) \times 4(N^2 - 1)$ matrix, representing the linear transformation

$$\Psi_\alpha \mapsto (\mathcal{M}\Psi)_\alpha \equiv (\Gamma_\mu)_{\alpha\beta} [A_\mu, \Psi_\beta], \quad (2.6)$$

acting on the linear space of traceless complex $N \times N$ matrices Ψ_α . The determinant $\det \mathcal{M}$ takes complex values in general and we define its phase Γ by $\det \mathcal{M} = |\det \mathcal{M}| e^{i\Gamma}$.

Eq. (2.3) becomes

$$Z = \int dA e^{-S_b} \det \mathcal{M} = \int dA e^{-S}, \quad (2.7)$$

where the effective action is

$$S = S_b - \ln \det \mathcal{M}. \quad (2.8)$$

In [11], it was shown that A_μ configurations that are close to d -dimensional configurations $3 \leq d \leq 6$ leads to milder fluctuations of Γ for smaller values of d . A “ d -dimensional configuration” is one that, by an appropriate $SO(6)$ transformation, we can set $A_{d+1} = \dots = A_6 = 0$. For $d = 2$, we have that $\det \mathcal{M} = 0$, showing that these configurations are suppressed in Eq. (2.7). This indicates that $SO(6)$ maybe broken down to $SO(3)$, but whether this is realized is a dynamical question depending on the competition with the larger entropy of configurations close to higher dimensional configurations. This question was addressed using the GEM in [38], where the free energy of the $SO(d)$ vacuum was calculated up to fifth order and it was found that the $SO(3)$ vacuum has the lowest free energy, which implies SSB to $SO(3)$. The extent of spacetime

$$\lambda_\mu = \frac{1}{N} \text{tr}(A_\mu)^2 \quad (2.9)$$

in the $SO(d)$ vacuum has expectation values $\langle \lambda_\mu \rangle$ which are large in d directions and small in the remaining $(6 - d)$ directions. This was calculated up to fifth order in the GEM and the result for the $SO(3)$ vacuum is

$$\langle \lambda_\mu \rangle \approx \begin{cases} 1.7 & \text{for the three extended directions,} \\ 0.2 & \text{for the three shrunken directions.} \end{cases} \quad (2.10)$$

3. The CLM Applied to the 6D Type IIB Matrix Model

The degrees of freedom in the model given by Eq. (2.7) are the Hermitian traceless matrices A_μ . The complex Langevin equation is the stochastic differential equation in the fictitious time t involving the *general complex* traceless matrices $A_\mu(t)$ [19, 20]

$$\frac{d(A_\mu)_{ij}(t)}{dt} = - \left. \frac{\partial S}{\partial (A_\mu)_{ji}} \right|_{A_\mu=A_\mu(t)} + (\eta_\mu)_{ij}(t), \quad (3.1)$$

where the $\eta_\mu(t)$ are traceless Hermitian matrices whose elements are random variables obeying the Gaussian distribution $\propto \exp\left(-\frac{1}{4} \int \text{tr}\{\eta_\mu(t)\}^2 dt\right)$ and S is the effective action (2.8). The drift term in the above equation is the term $-\partial S/\partial(A_\mu)_{ji}$, which is given explicitly by

$$\frac{\partial S}{\partial (A_\mu)_{ji}} = \frac{\partial S_b}{\partial (A_\mu)_{ji}} - \text{Tr} \left(\frac{\partial \mathcal{M}}{\partial (A_\mu)_{ji}} \mathcal{M}^{-1} \right), \quad (3.2)$$

where Tr represents the trace of a $4(N^2 - 1) \times 4(N^2 - 1)$ matrix. The second term in the above equation is not Hermitian, which makes the use of general complex traceless matrices $A_\mu(t)$ necessary. The expectation value $\langle \mathcal{O}[A_\mu] \rangle$ of an observable $\mathcal{O}[A_\mu]$,

$$\langle \mathcal{O}[A_\mu] \rangle = \frac{1}{Z} \int dA e^{-S}, \quad (3.3)$$

can be calculated from a solution of Eq. (3.2) from

$$\langle \mathcal{O}[A_\mu] \rangle = \frac{1}{T} \int_{t_0}^{t_0+T} \mathcal{O}[A_\mu(t)] dt, \quad (3.4)$$

where t_0 is the thermalization time and T is large enough in order to obtain satisfactory statistics.

In order for the Eq. (3.3) and Eq. (3.4) to give the same result, the probability distribution $P(A_\mu^{(R)}, A_\mu^{(I)}; t)$ of the (general complex traceless matrix) solutions $A_\mu(t)$ of Eq. (3.1), where $A_\mu^{(R)}(t) = (A_\mu(t) + A_\mu^\dagger(t))/2$, $A_\mu^{(I)}(t) = (A_\mu(t) - A_\mu^\dagger(t))/2i$, must satisfy the relation

$$\int dA_\mu \rho(A_\mu; t) \mathcal{O}[A_\mu] = \int dA_\mu^{(R)} dA_\mu^{(I)} P(A_\mu^{(R)}, A_\mu^{(I)}; t) \mathcal{O}[A_\mu^{(R)} + iA_\mu^{(I)}]. \quad (3.5)$$

On the LHS of the above equation, A_μ are the original Hermitian matrices in the model given by Eq. (2.7) and $\rho(A_\mu; t)$ is a complex weight which is a solution of a Fokker-Planck equation, such that $\lim_{t \rightarrow \infty} \rho(A_\mu; t) = e^{-S}/Z$, giving the desired $\langle \mathcal{O}[A_\mu] \rangle$ in the $t \rightarrow \infty$ limit. On the RHS of Eq. (3.5), we have the (real positive) probability distribution $P(A_\mu^{(R)}, A_\mu^{(I)}; t)$ of the complex matrix solutions $A_\mu(t)$ of Eq. (3.1) and the analytic continuation of $\mathcal{O}[A_\mu] \mapsto \mathcal{O}[A_\mu^{(R)} + iA_\mu^{(I)}]$. For large enough t , the RHS of Eq. (3.5) is calculated using the RHS of Eq. (3.4). A necessary and sufficient condition for the equality in Eq. (3.4) to hold is that the probability distribution of

$$u = \sqrt{\frac{1}{6N^3} \sum_{\mu=1}^6 \sum_{i,j=1}^N \left| \frac{\partial S}{\partial (A_\mu)_{ij}} \right|^2}, \quad (3.6)$$

in $P(A^{(R)}, A^{(I)}; t)$ falls off exponentially or faster [24]. There are two basic reasons for violating this condition. The first one is the “excursion problem”, where the solutions of Eq. (3.1) drift deep into the anti-Hermitian direction. The second one is the “singular drift problem”, which occurs due to the appearance of \mathcal{M}^{-1} in Eq. (3.2) when some eigenvalues of \mathcal{M} accumulate near zero frequently.

The excursion problem can be avoided by using the gauge cooling technique [27]. We minimize the “Hermitian norm”

$$\mathcal{N}_H(t) = -\frac{1}{6N} \sum_{\mu=1}^6 \text{tr} \left\{ (A_\mu(t) - A_\mu(t)^\dagger)^2 \right\}, \quad (3.7)$$

by performing an $\text{SL}(N, \mathbb{C})$ transformation $A_\mu(t) \mapsto g(t)A_\mu g(t)^{-1}$, where $g(t) = \exp\{-\alpha G(t)\}$ and $G(t) = \frac{1}{N} \sum_{\mu=1}^6 [A_\mu(t), A_\mu(t)^\dagger]$. $G(t)$ is the gradient of $\mathcal{N}_H(t)$ wrt the $\text{SL}(N, \mathbb{C})$ transformation [31]. The real positive parameter α is computed so that $\mathcal{N}_H(t)$ is minimized. In [24, 28], it was shown that gauge cooling does not affect the argument for the justification of the CLM.

The singular drift problem can be avoided by deforming the fermionic action by adding the term

$$\Delta S_f = N m_f \text{tr} (\bar{\Psi}_\alpha (\Gamma_6)_{\alpha\beta} \Psi_\beta) \quad (3.8)$$

to the action, so that $S_f \mapsto S_f + \Delta S_f$. $m_f \geq 0$ is the deformation parameter. This term modifies the matrix \mathcal{M} of Eq. (2.6), so that

$$\Psi_\alpha \mapsto (\mathcal{M}\Psi)_\alpha \equiv (\Gamma_\mu)_{\alpha\beta} [A_\mu, \Psi_\beta] + m_f \Psi_\alpha, \quad (3.9)$$

and shifts its eigenvalues in the real direction. A typical case is shown in figure 1. This method was successfully applied in [31] in an $\text{SO}(4)$ symmetric matrix model with a complex fermion determinant and a severe complex action problem. For m_f large enough, the eigenvalues of \mathcal{M}

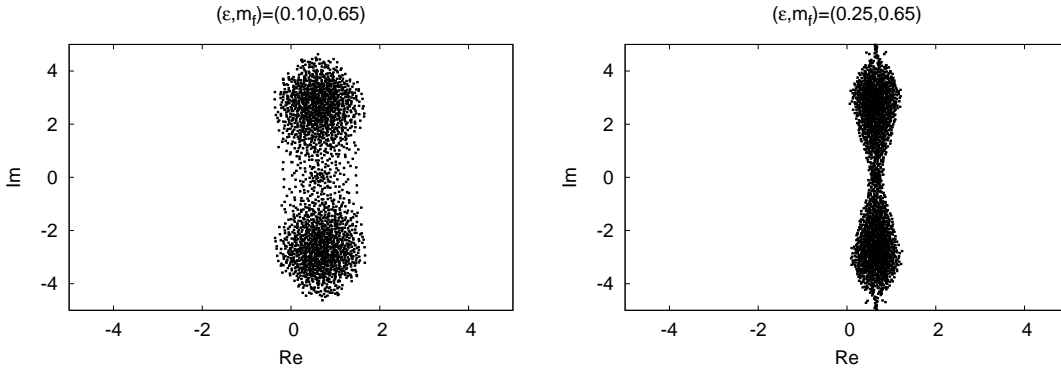


Figure 1: The effect of the deformation ΔS_f of Eq. (3.8) on the eigenvalues of the matrix \mathcal{M} for a typical configuration for $N = 24$, $m_f = 0.65$, $\varepsilon = 0.10$ (Left) and $\varepsilon = 0.25$ (Right). By increasing m_f , the eigenvalues shift in the direction of the real axis. Notice also that by increasing ε for given m_f , the spread of the eigenvalues in the real direction decreases.

avoid zero and we don’t have the singular drift problem. This term breaks the $\text{SO}(6)$ symmetry

down to $\text{SO}(5)$. Since we are looking for $\text{SO}(d)$ SSB patterns with $d < 5$, this is not a problem. In the end, the $m_f \rightarrow 0$ limit will be taken in order to obtain the $D = 6$ IIB model. Assuming that nothing dramatic happens in the $m_f = 0$ region, the extrapolation from the region of small m_f will give the correct pattern of SSB of the undeformed model, as it happened in [31], where the expected $\text{SO}(4)$ to $\text{SO}(2)$ breaking was observed. When $m_f \rightarrow \infty$, the fermions decouple and we obtain a matrix model with only bosonic degrees of freedom. In this case, it is known that the $\text{SO}(6)$ symmetry is not broken [7]. Therefore, the deformation parameter m_f can be seen as interpolating between the bosonic matrix model and the $D = 6$ IIB model.

The numerical solution of Eq. (3.1) is computed by discretizing the fictitious time t

$$(A_\mu)_{ij}(t + \Delta t) = (A_\mu)_{ij}(t) - \Delta t \frac{\partial \mathcal{S}}{\partial (A_\mu)_{ji}} \Big|_{A_\mu = A_\mu(t)} + \sqrt{\Delta t} (\eta_\mu)_{ij}(t). \quad (3.10)$$

The $\sqrt{\Delta t}$ comes from the chosen normalization of the $\eta_\mu(t) \propto \exp\left(-\frac{1}{4} \sum_j \text{tr}\{\eta_\mu(t)\}^2\right)$. The step-size Δt is chosen adaptively, so that the drift term remains small [41]. The details of the numerical computation can be found in [37].

The order parameters of the SSB are taken to be the spacetime extensions in the μ -direction

$$\lambda_\mu = \frac{1}{N} \text{tr} (A_\mu)^2, \quad (3.11)$$

where no sum over μ is taken. In order to calculate $\langle \lambda_\mu \rangle$, we add the term

$$\Delta \mathcal{S}_b = \frac{1}{2} N \varepsilon \sum_{\mu=1}^6 m_\mu \text{tr} (A_\mu)^2 \quad (3.12)$$

to the action, so that $\mathcal{S}_b \mapsto \mathcal{S}_b + \Delta \mathcal{S}_b$, where we take $0 < m_1 \leq \dots \leq m_6$ and $\varepsilon > 0$. This term breaks the $\text{SO}(6)$ symmetry explicitly, and SSB is probed by first taking the large- N limit and then sending $\varepsilon \rightarrow 0$. Notice that, although $\lambda_\mu(t)$ is not real for a configuration $A_\mu(t)$, the expectation values $\langle \lambda_\mu \rangle$ are real due to the symmetry of the drift term (3.2) under $A_i \mapsto A_i^\dagger$ for $i = 1, \dots, 5$ and $A_6 \mapsto -A_6^\dagger$. Due to the chosen ordering of the m_μ , we will have that

$$\langle \lambda_1 \rangle \geq \langle \lambda_2 \rangle \geq \dots \geq \langle \lambda_6 \rangle. \quad (3.13)$$

When we take the large- N limit and then $\varepsilon \rightarrow 0$ and find that the $\langle \lambda_\mu \rangle$ are not equal, we conclude that the $\text{SO}(6)$ symmetry is spontaneously broken. For finite m_f , SSB occurs if we find that some of the $\langle \lambda_\mu \rangle$ are not equal for $\mu = 1, \dots, 5$.

In this work, we take

$$m_\mu = (0.5, 0.5, 1, 2, 4, 8). \quad (3.14)$$

This choice retains the $\text{SO}(2)$ symmetry, but since we do not expect the SSB to $\text{SO}(2)$ to occur, this is not a problem. It is preferable to keep the spectrum of the m_μ not too wide in order to take the $\varepsilon \rightarrow 0$ extrapolation without introducing large systematic errors.

4. Results

To summarize, the model that we investigate numerically using the CLM is given by Eq. (3.10), where we have taken $S \mapsto S + \Delta S_b + \Delta S_f$. We use (3.4) to compute the expectation values $\langle \lambda_\mu \rangle_{m_f, \varepsilon, N}$. In order to check for the large excursion and singular drift problems, we measure the norm \mathcal{N}_H of Eq. (3.7) and the magnitude of the drift u of Eq. (3.6) and plot their histograms and time histories. In figure 2 we plot the histogram $p(u)$ for $N = 24$ and $m_f = 0.65, 0.90$. For

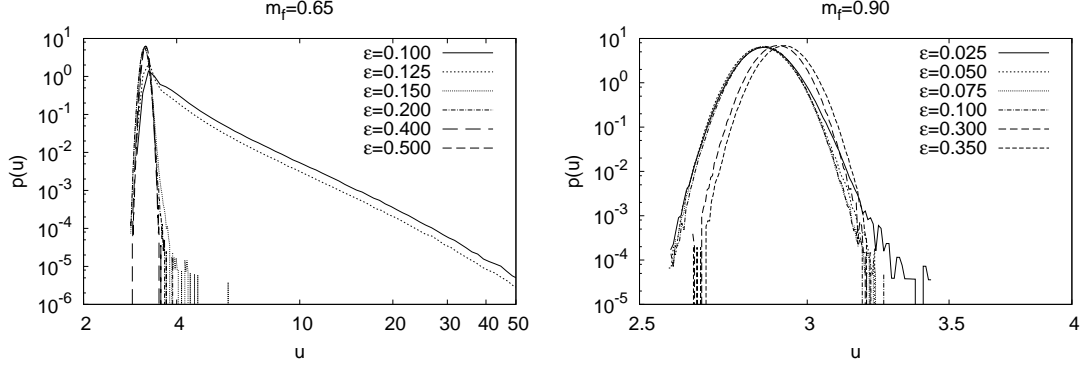


Figure 2: The probability distribution $p(u)$ of u defined in Eq. (3.6) for $N = 24$ with $m_f = 0.65$ (Left) and $m_f = 0.90$ (Right).

$m_f = 0.65$, we see that $p(u)$ falls off exponentially or faster for $\varepsilon \geq 0.150$, whereas it develops a power-law tail for $\varepsilon \leq 0.125$. Therefore, we can trust only the results for $\varepsilon \geq 0.150$. For $m_f = 0.90$ we see that no power law tail exists for all values of ε investigated.

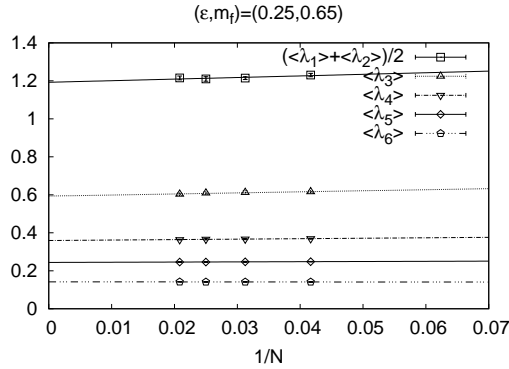


Figure 3: The expectation values $\langle \lambda_\mu \rangle_{m_f, \varepsilon, N}$ for $m_f = 0.65$, $\varepsilon = 0.25$ and $N = 24, 32, 40, 48$ together with a fit of the form $a + b/N$. The fit is used for the large- N extrapolation discussed in the text and the fitting parameter a gives $\langle \lambda_\mu \rangle_{m_f, \varepsilon} = \lim_{N \rightarrow \infty} \langle \lambda_\mu \rangle_{m_f, \varepsilon, N}$.

In order to probe the SSB, first we have to take the large- N limit $\langle \lambda_\mu \rangle_{m_f, \varepsilon} = \lim_{N \rightarrow \infty} \langle \lambda_\mu \rangle_{m_f, \varepsilon, N}$. For that, we plot $\langle \lambda_\mu \rangle_{m_f, \varepsilon, N}$ as a function of $1/N$, as in figure 3. We consider the average $(\langle \lambda_1 \rangle + \langle \lambda_2 \rangle)/2$ instead of $\langle \lambda_1 \rangle$ and $\langle \lambda_2 \rangle$ separately due to the choice (3.14) and in order to increase statistics. The large- N extrapolation is done by fitting the data to a linear form $a + b/N$. Our data fits nicely for all values of (m_f, ε) considered and for $24 \leq N \leq 48$ and the coefficient a gives $\langle \lambda_\mu \rangle_{m_f, \varepsilon}$.

Then we have to take the $\varepsilon \rightarrow 0$ limit. We compute the ratio [31]

$$\rho_\mu(m_f, \varepsilon) = \frac{\langle \lambda_\mu \rangle_{m_f, \varepsilon}}{\sum_{\nu=1}^6 \langle \lambda_\nu \rangle_{m_f, \varepsilon}}, \quad (4.1)$$

instead of $\langle \lambda_\mu \rangle_{m_f, \varepsilon}$, because some of the finite ε effects cancel between the numerator and the denominator. In figure 4 we show the plots of $\rho_\mu(m_f, \varepsilon)$ as a function of ε for $m_f = 0.65, 1.00, 1.40, 1000$.

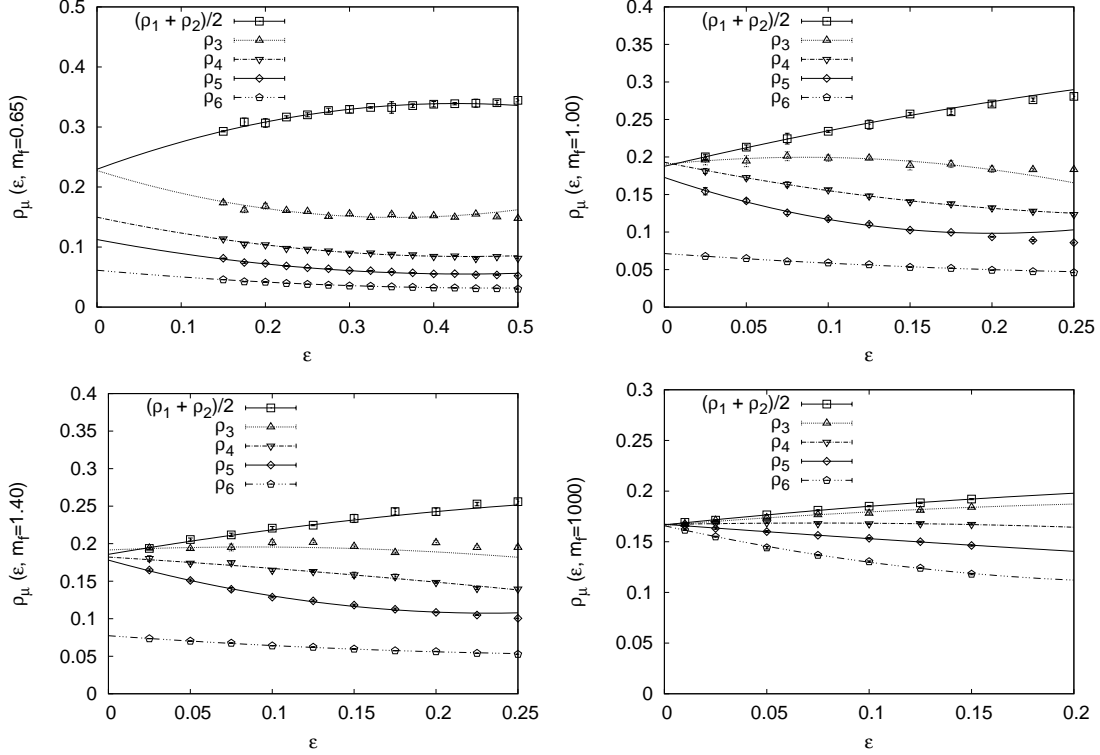


Figure 4: The ratio $\rho_\mu(m_f, \varepsilon)$ defined in Eq. (4.1) as a function of ε for $m_f = 0.65$ (Top-Left), $m_f = 1.00$ (Top-Right), $m_f = 1.40$ (Bottom-Left) and $m_f = 1000$ (Bottom-Right). Only the values of ε where the singular drift problem is absent are shown. The lines are a fit to $a + b\varepsilon + c\varepsilon^2$.

We plot only the data that do not suffer from the singular drift problem by applying the criterion of exponential or faster suppression of the tail of $p(u)$ (see figure 2). We also consider the average $(\rho_1 + \rho_2)/2$ instead of ρ_1 and ρ_2 due to the choice (3.14) and in order to reduce statistical errors. The $\varepsilon \rightarrow 0$ extrapolation is done by fitting our data to a quadratic function $a + b\varepsilon + c\varepsilon^2$ and the fitting parameter a gives

$$\rho_\mu(m_f) = \lim_{\varepsilon \rightarrow 0} \rho_\mu(m_f, \varepsilon). \quad (4.2)$$

The fitting ranges that satisfy the singular drift problem criterion and fit well to this function are $0.150 \leq \varepsilon \leq 0.475$ for $m_f = 0.65$, $0.025 \leq \varepsilon \leq 0.175$ for $m_f = 1.00$, $0.025 \leq \varepsilon \leq 0.200$ for $m_f = 1.40$, $0.010 \leq \varepsilon \leq 0.150$ for $m_f = 1000$. For $m_f = 0.65$ we see that the curves $(\rho_1 + \rho_2)/2$ and ρ_3 intersect at $\varepsilon = 0$, implying that the $SO(5)$ symmetry of the deformed model is spontaneously broken to $SO(3)$. For $m_f = 1.00$ we see that the curves $(\rho_1 + \rho_2)/2$, ρ_3 and ρ_4 intersect at $\varepsilon = 0$,

implying that the $SO(5)$ symmetry of the deformed model is spontaneously broken to $SO(4)$. For $m_f = 1.40$ we see that the curves $(\rho_1 + \rho_2)/2$, ρ_3 , ρ_4 and ρ_5 intersect at $\varepsilon = 0$, implying that the $SO(5)$ symmetry is not spontaneously broken. Finally, for $m_f = 1000$, all the ρ_μ curves intersect at $\varepsilon = 0$, implying that the $SO(6)$ symmetry is not spontaneously broken. This is consistent with the fact that at $m_f \rightarrow \infty$ the fermions decouple and the deformed model reduces to the bosonic matrix model.

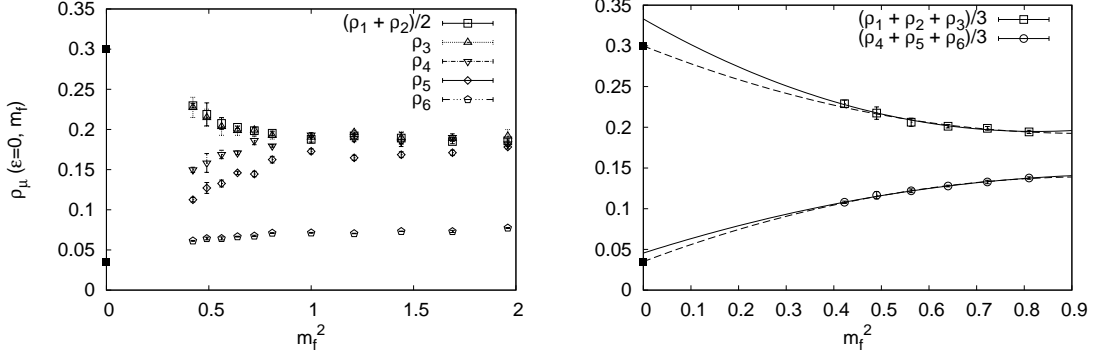


Figure 5: (Left) The values $\rho(m_f)$ of Eq. (4.2) as a function of m_f^2 for $m_f = 0.65, 0.70, 0.75, 0.80, 0.85, 0.90, 1.0, 1.10, 1.20, 1.30, 1.40$. The filled squares are the GEM predictions of Eq. (4.3). (Right) The averages $(\rho_1 + \rho_2 + \rho_3)/3$ and $(\rho_4 + \rho_5 + \rho_6)/3$ as a function of m_f^2 for $m_f \leq 0.9$, corresponding to the $SO(3)$ symmetric phase. The solid lines are fits to $a + bm_f^2 + cm_f^4$ and the dashed lines are similar fits constrained to pass through the $m_f = 0$ points (4.3) predicted by GEM.

Finally, we consider the $m_f \rightarrow 0$ limit, which will give the undeformed $D = 6$ IIB matrix model. In figure 5 we plot the values $\rho_\mu(m_f)$ of Eq. (4.2). We see that an $SO(3)$ vacuum develops for $m_f \lesssim 0.90$, whereas an $SO(4)$ vacuum develops for $1.00 \lesssim m_f \lesssim 1.30$. Considering the fact that an $SO(2)$ vacuum does not realize due to the vanishing $\det \mathcal{M}$, we conclude that as $m_f \rightarrow 0$ the $SO(3)$ vacuum survives. We conclude that in the undeformed model $m_f = 0$, the $SO(6)$ rotational symmetry is spontaneously broken to $SO(3)$, in agreement with the GEM prediction.

From Eq. (2.10) we obtain

$$\rho_1 = \rho_2 = \rho_3 \simeq \frac{1.7}{5.7} \simeq 0.3, \quad \rho_4 \simeq \rho_5 \simeq \rho_6 \simeq \frac{0.2}{5.7} \simeq 0.035. \quad (4.3)$$

These values are put in the plots of figure 5. The left plot of figure 5 shows the averages $(\rho_1 + \rho_2 + \rho_3)/3$ and $(\rho_4 + \rho_5 + \rho_6)/3$ as a function of m_f^2 for $m_f \leq 0.9$, corresponding to the $SO(3)$ symmetric phase. Due to the symmetry $m_f \mapsto -m_f$, as $m_f \rightarrow 0$, the asymptotic behavior of these functions is expected to be a power series in m_f^2 . We fit the corresponding data to a polynomial $a + bm_f^2 + cm_f^4$ for $0.65 \leq m_f \leq 0.90$. The $m_f \rightarrow 0$ extrapolation gives

$$\frac{\rho_1 + \rho_2 + \rho_3}{3} = 0.33(2), \quad \frac{\rho_4 + \rho_5 + \rho_6}{3} = 0.046(3), \quad (4.4)$$

which are close to the values (4.3) predicted by the GEM. We should note that the GEM has systematic errors due to the truncations involved in the calculations. Therefore we conclude that

the results calculated by the CLM Eq. (4.4) are in reasonable quantitative agreement with the GEM results of Eq. (4.3).

Acknowledgements

We thank H. Kawai and H. Steinacker for valuable comments and discussions. This research was supported by MEXT as “Priority Issue on Post-K computer” (Elucidation of the Fundamental Laws and Evolution of the Universe) and Joint Institute for Computational Fundamental Science (JICFuS). Computations were carried out using computational resources such as KEKCC, the NTUA het clusters, the FX10 at Kyushu University. This work was also supported by computational time granted from the Greek Research & Technology Network (GRNET) in the National HPC facility - ARIS - under project ID IKKT10D. T. A. was supported in part by Grant-in-Aid for Scientific Research (No. 17K05425) from Japan Society for the Promotion of Science.

References

- [1] N. Ishibashi, H. Kawai, Y. Kitazawa and A. Tsuchiya, Nucl. Phys. B **498** (1997) 467 doi:10.1016/S0550-3213(97)00290-3 [hep-th/9612115]. For a review, see e.g. H. Aoki, S. Iso, H. Kawai, Y. Kitazawa, A. Tsuchiya and T. Tada, Prog. Theor. Phys. Suppl. **134** (1999) 47 doi:10.1143/PTPS.134.47 [hep-th/9908038].
- [2] S. W. Kim, J. Nishimura and A. Tsuchiya, Phys. Rev. Lett. **108** (2012) 011601 doi:10.1103/PhysRevLett.108.011601 [arXiv:1108.1540 [hep-th]].
- [3] T. Aoki, M. Hirasawa, Y. Ito, J. Nishimura and A. Tsuchiya, arXiv:1904.05914 [hep-th].
- [4] J. Nishimura and A. Tsuchiya, arXiv:1904.05919 [hep-th].
- [5] J. Nishimura, T. Okubo and F. Sugino, JHEP **1110** (2011) 135 doi:10.1007/JHEP10(2011)135 [arXiv:1108.1293 [hep-th]].
- [6] W. Krauth, H. Nicolai and M. Staudacher, Phys. Lett. B **431** (1998) 31 doi:10.1016/S0370-2693(98)00557-7 [hep-th/9803117].
- [7] T. Hotta, J. Nishimura and A. Tsuchiya, Nucl. Phys. B **545** (1999) 543 doi:10.1016/S0550-3213(99)00056-5 [hep-th/9811220].
- [8] J. Ambjorn, K. N. Anagnostopoulos, W. Bietenholz, T. Hotta and J. Nishimura, JHEP **0007** (2000) 013 doi:10.1088/1126-6708/2000/07/013 [hep-th/0003208].
- [9] J. Ambjorn, K. N. Anagnostopoulos, W. Bietenholz, T. Hotta and J. Nishimura, JHEP **0007** (2000) 011 doi:10.1088/1126-6708/2000/07/011 [hep-th/0005147].
- [10] J. Ambjorn, K. N. Anagnostopoulos, W. Bietenholz, F. Hofheinz and J. Nishimura, Phys. Rev. D **65** (2002) 086001 doi:10.1103/PhysRevD.65.086001 [hep-th/0104260].
- [11] J. Nishimura and G. Vernizzi, JHEP **0004** (2000) 015 doi:10.1088/1126-6708/2000/04/015 [hep-th/0003223].
- [12] J. Nishimura and G. Vernizzi, Phys. Rev. Lett. **85** (2000) 4664 doi:10.1103/PhysRevLett.85.4664 [hep-th/0007022].
- [13] K. N. Anagnostopoulos and J. Nishimura, Phys. Rev. D **66** (2002) 106008 doi:10.1103/PhysRevD.66.106008 [hep-th/0108041].

- [14] J. Nishimura, Phys. Rev. D **65** (2002) 105012 doi:10.1103/PhysRevD.65.105012 [hep-th/0108070].
- [15] K. N. Anagnostopoulos, T. Azuma and J. Nishimura, Phys. Rev. D **83** (2011) 054504 doi:10.1103/PhysRevD.83.054504 [arXiv:1009.4504 [cond-mat.stat-mech]].
- [16] K. N. Anagnostopoulos, T. Azuma and J. Nishimura, JHEP **1110** (2011) 126 doi:10.1007/JHEP10(2011)126 [arXiv:1108.1534 [hep-lat]].
- [17] K. N. Anagnostopoulos, T. Azuma and J. Nishimura, JHEP **1311** (2013) 009 doi:10.1007/JHEP11(2013)009 [arXiv:1306.6135 [hep-th]].
- [18] K. N. Anagnostopoulos, T. Azuma and J. Nishimura, PoS LATTICE **2015** (2016) 307 doi:10.22323/1.251.0307 [arXiv:1509.05079 [hep-lat]].
- [19] G. Parisi, *On complex probabilities*, Phys. Lett. B **131** (1983) 393.
- [20] J. R. Klauder, *Coherent state Langevin equations for canonical quantum systems with applications to the quantized Hall effect*, Phys. Rev. A **29** (1984) 2036.
- [21] G. Aarts, E. Seiler and I. O. Stamatescu, Phys. Rev. D **81** (2010) 054508 doi:10.1103/PhysRevD.81.054508 [arXiv:0912.3360 [hep-lat]].
- [22] G. Aarts, F. A. James, E. Seiler and I. O. Stamatescu, Eur. Phys. J. C **71** (2011) 1756 doi:10.1140/epjc/s10052-011-1756-5 [arXiv:1101.3270 [hep-lat]].
- [23] J. Nishimura and S. Shimasaki, Phys. Rev. D **92** (2015) no.1, 011501 doi:10.1103/PhysRevD.92.011501 [arXiv:1504.08359 [hep-lat]].
- [24] K. Nagata, J. Nishimura and S. Shimasaki, Phys. Rev. D **94** (2016) no.11, 114515 doi:10.1103/PhysRevD.94.114515 [arXiv:1606.07627 [hep-lat]].
- [25] L. L. Salcedo, Phys. Rev. D **94** (2016) no.11, 114505 doi:10.1103/PhysRevD.94.114505 [arXiv:1611.06390 [hep-lat]].
- [26] G. Aarts, E. Seiler, D. Sexty and I. O. Stamatescu, JHEP **1705** (2017) 044 Erratum: [JHEP **1801** (2018) 128] doi:10.1007/JHEP05(2017)044, 10.1007/JHEP01(2018)128 [arXiv:1701.02322 [hep-lat]].
- [27] E. Seiler, D. Sexty and I. O. Stamatescu, Phys. Lett. B **723** (2013) 213 doi:10.1016/j.physletb.2013.04.062 [arXiv:1211.3709 [hep-lat]].
- [28] K. Nagata, J. Nishimura and S. Shimasaki, PTEP **2016** (2016) no.1, 013B01 doi:10.1093/ptep/ptv173 [arXiv:1508.02377 [hep-lat]].
- [29] S. Tsutsui and T. M. Doi, Phys. Rev. D **94** (2016) no.7, 074009 doi:10.1103/PhysRevD.94.074009 [arXiv:1508.04231 [hep-lat]].
- [30] K. Nagata, J. Nishimura and S. Shimasaki, JHEP **1607** (2016) 073 doi:10.1007/JHEP07(2016)073 [arXiv:1604.07717 [hep-lat]].
- [31] Y. Ito and J. Nishimura, JHEP **1612** (2016) 009 doi:10.1007/JHEP12(2016)009 [arXiv:1609.04501 [hep-lat]].
- [32] J. Bloch, Phys. Rev. D **95** (2017) no.5, 054509 doi:10.1103/PhysRevD.95.054509 [arXiv:1701.00986 [hep-lat]].
- [33] T. M. Doi and S. Tsutsui, Phys. Rev. D **96** (2017) no.9, 094511 doi:10.1103/PhysRevD.96.094511 [arXiv:1709.05806 [hep-lat]].

- [34] J. Bloch, J. Glesaaen, J. J. M. Verbaarschot and S. Zafeiropoulos, *JHEP* **1803** (2018) 015
doi:10.1007/JHEP03(2018)015 [arXiv:1712.07514 [hep-lat]].
- [35] J. Nishimura, T. Okubo and F. Sugino, *Prog. Theor. Phys.* **114** (2005) 487 doi:10.1143/PTP.114.487
[hep-th/0412194].
- [36] A. Mollgaard and K. Splittorff, *Phys. Rev. D* **88** (2013) no.11, 116007
doi:10.1103/PhysRevD.88.116007 [arXiv:1309.4335 [hep-lat]].
- [37] K. N. Anagnostopoulos, T. Azuma, Y. Ito, J. Nishimura and S. K. Papadoudis, *JHEP* **1802** (2018) 151
doi:10.1007/JHEP02(2018)151 [arXiv:1712.07562 [hep-lat]].
- [38] T. Aoyama, J. Nishimura and T. Okubo, *Prog. Theor. Phys.* **125** (2011) 537 doi:10.1143/PTP.125.537
[arXiv:1007.0883 [hep-th]].
- [39] K. N. Anagnostopoulos, T. Azuma, Y. Ito, J. Nishimura, T. Okubo and S. K. Papadoudis, work in progress.
- [40] K. Nagata, J. Nishimura and S. Shimasaki, *EPJ Web Conf.* **175** (2018) 07017
doi:10.1051/epjconf/201817507017 [arXiv:1710.07416 [hep-lat]].
- [41] G. Aarts, F. A. James, E. Seiler and I. O. Stamatescu, *Phys. Lett. B* **687** (2010) 154
doi:10.1016/j.physletb.2010.03.012 [arXiv:0912.0617 [hep-lat]].